

# Experimental investigation into brick masonry arches' (vault and rib cover) behavior reinforced by FRP strips under vertical load

Majid Reza Takbash<sup>a</sup>, Abbas Ali Akbarzadeh Morshedi\* and Seyyed Ali Sabet<sup>b</sup>

Department of Civil Engineering, Kashan Branch, Islamic Azad University, Kashan, Iran

(Received January 17, 2018, Revised June 6, 2018, Accepted June 7, 2018)

**Abstract.** The current experimental study is the reinforcement of the simple curvature vault masonry structures. In this study, we discuss complex structure include vault and rib cover with two radii and actual dimensions under a vertical load. The unreinforced structure data were compared with analysis data. The analysis data are in good agreement with experimental data. In the first experiment, a structure without reinforcement is tested and according to the test results, the second structure was reinforced using the carbon polymer fibers and the same test is done to see the effects of reinforcement. Based on the test results of the first structure, the first cracks are created in the vault. Moreover, the reinforcement with carbon fibers will increase the loading capacity of the structure around 35%.

**Keywords:** brick masonry arches; experimental tests; FRP; structural reinforcements; vault and rib cover

## 1. Introduction

Numerous historical constructions are still in service all over the world, and a significant number of them are of cultural and artistic value. Many historical constructions contain masonry arches and domes. Masonry arches are typical components of historic buildings throughout the world, and their damage or collapse is very often caused by earthquakes. The first-order seismic assessment of masonry structures can be represented by the equivalent static analysis method, which does not capture all of the dynamics, but provides a measure of the lateral loading that the structure can withstand before collapse (Dimitri *et al.* 2015). In the evaluation of the vulnerability of built cultural heritage, a comprehensive literature addresses circular arches, while few works consider pointed arches and none of them deals with seismic actions (Misseri *et al.* 2017). These historical sites as a cultural heritage should be protected for the next generation and this shows the importance of research in this area. Since these structures are not strong against the tensile and shear forces, any vertical load or earthquake can cause a problem for them. As a result, some enhancement and repair techniques are required to reestablish their performances and to prevent the brittle collapse of the masonry as an important part of them. A structure consists of vault and rib cover is a common structure in the historical sites especially in the Middle East. The maintenance and reinforcement of these structures

should be done based on their service load. With attention to the many issues linked to the maintenance and restoration of historic buildings (ICOMOS 2013), the interest of researchers in this field is devoted increasingly to the development of innovative materials and advanced technologies. Specifically, there are increasing interests in fiber-reinforced polymer (FRP) composites that are used in the structural reinforcement for more than a decade (Fanning and Kelly 1999, Nanni 1993, Smith and Teng 2002). The arches in the masonry of the existing building are unprotected and they are not strong enough due to insufficient strength properties of materials. To improve these structures, structural behavior and mechanisms of collapse of historic structures should be analyzed. The CNR-DT200/2004 standards suggest using the carbon fiber reinforced polymer (CFRP) strip directly either at the intrados or at the extrados of the vault at simple curvature to reduce the number of plastic hinge during collapse mechanism. The best technique is using the strips on both sides of the vault. In the case of the barrel vault, the reinforcement should be uniformly applied along the directrix with a suggested step. Some studies carried out on the barrel vaults showed the vulnerability of the CFRP extrados strengthening in terms of shear collapse due to the peeling (Lourenço and Oliveira 2006, Valluzzi *et al.* 2001, Foraboschi 2004, Creazza *et al.* 2001, Capozucca 2007, Aiello and Sciolti 2008).

There are different methods to strengthen these coatings, such as using a combination of steel and concrete. Because of the failure to maintain traditional systems, architectural and structural damage occurs. Some outstanding features of FRP like, low weight, high strength, easy handling and desired flexibility with minimal changes to the structure encourage researchers to use this material. Moreover, the use of these materials does not alter the natural behavior of the structure since they do not add mass. In addition, they are removable, and they can be made either invisible or

\*Corresponding author, Assistant Professor

E-mail: A.Akbarzadeh@iaukashan.ac.ir

<sup>a</sup>M.Sc. Student

E-mail: majid\_takbash@yahoo.com

<sup>b</sup>Scientific Board

E-mail: Sabet@iaukashan.ac.ir

visible, to comply with modern restoration requirements. CFRP composite materials have been widely used to strengthen masonry constructions. The bond between CFRP and substrate strongly conditions the performance of the reinforced masonry structures. Characterization of the shear bond mechanical behavior of masonry-CFRP interface thus becomes a crucial factor. FRPs are accepted as an efficient material for the external strengthening of masonry structures. Previous works have shown that the bond between FRP and the substrate plays an important role in the effectiveness of this strengthening technique. Extensive investigations have been devoted to the characterization of the short-term bond behavior, while its durability and long-term performance requires further studies. (Basilio *et al.* 2004, Borri *et al.* 2009, De Lorenzis *et al.* 2007, Rotunno *et al.* 2014, (Ghiassi *et al.* 2014). Reinforcement often changes the location of cracks and delay it. As found in De Lorenzis *et al.* (2007), Briccoli Bati and Rovero (2008) and Foraboschi (2004), the use of composite materials enables the masonry structures to carry substantial tensile stresses and eliminating their greatest mechanical shortcoming at an acceptable cost. More specifically, reinforcement is incapable of preventing masonry from cracking (to do so, it would either have to have a stiffness several times greater than the masonry, or it would have to be pre-stressed), but it does transmit the tension force between the two faces of the crack, i.e., it stitches the crack. Hence cracks may form at a reinforced boundary, but cannot open, since the tension force is transmitted by the reinforcement in lieu of the cracked masonry, i.e., the tension force bypasses the cracks and passes into the reinforcement. This means that reinforcing the extrados or the intrados of the vault allows preventing all mechanisms (hinged mode failures) from occurring, forcing such structures to fail by other failure modes (i.e., crushing, sliding, debonding or FRP rupture). Parametric analyses have been developed for predicting the ultimate load associated with each failure modes, the lowest of which constitutes the strength of the reinforced masonry arch (Briccoli Bati and Rovero 2008, Foraboschi 2004). According to such analysis and the abovementioned experimental studies, when FRP strips are bonded at the intrados, the effectiveness of the strengthening scheme was found to be highly dependent on the bond between the composite strip and existing structure. In the presence of concavely-curved soffits, the FRP laminates tend to get straightened under tension, leading to a multiaxial stress state, which combines the shear stresses ( $\tau$ ), parallel to the bonding masonry boundary, with transverse tensile stresses ( $\sigma$ ), which accelerate debonding failure (De Lorenzis and Zavarise 2009, Eshwar *et al.* 2005). Under such conditions, peeling and debonding became critical considerations in the design of masonry arches strengthening since the load-carrying capacity for this failure mode is commonly much lower than that of the other failure modes (Borri *et al.* 2009). The damage consists in a notch that reduces the height of the cross-section at a given abscissa and therefore causes a variation in the flexural stiffness of the structure. The analytical values of static displacements due to applied loads are calculated by means of the principle of virtual work for both the undamaged and damaged arch (Annalisa Greco *et al.* 2011). Masonry arch bridges present a large segment of Iranian railway bridge stock. The ever-increasing trend in traffic requires constant health

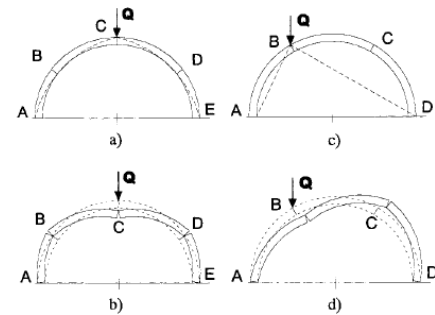


Fig. 1 Line of thrust and collapse mechanism of unreinforced arch subjected to vertical load applied to: (a, b) middle of arch span; (c, d) 1/4 of arch span (Valluzzi *et al.* 2001)

monitoring of such structures to determine their load carrying capacity and life expectancy (Shervan Ataei *et al.* 2016). A series of tests on full-scale brick masonry panels under biaxial compression has been performed in limited principal stress ratios oriented at various angles to the bed joints. Failure modes of tested panels were observed and failure features were analyzed to reveal the mechanical behavior of masonry under biaxial compression (Ren Xin *et al.* 2017).

This study examined the behavior of masonry vault under vertical loading applied to 1/4 of the span of the structure until the ultimate strength and how to change behavior in the presence of reinforcement, the vertical load is investigated. The difference of vault and rib cover made Relative to other tasks that structures tested in accordance with Iran's arch implemented in most historic buildings. The arc of vaults and rib cover is kind of six-part with two radii. Two samples of vault and rib cover built with actual dimensions and at the first time, the structures without any reinforcement tested then the second structure reinforced with FRP and loaded.

## 2. Analysis of behavior of vaults

### 2.1 Unreinforced masonry vaults

The stability and the safety of curved structures under a given loading condition are strongly dependent on the geometry of the structures and the mechanical characteristics of the constituent material. The masonry has a low tensile strength, so the safety condition for masonry arches (or vaults) is achieved when the line of thrust, coincident with the funicular polygon, is kept inside of each section of the arch. When the resultant of the internal forces move towards the outside of the central core, the section particles and a phase of high deformations start. The consequence of this is the formation of a plastic hinge. Fig. 1 shows the trend of the line of thrust and the failure pattern of an unreinforced arch under two different loading conditions. The vertical load  $Q$  concentrated in the middle of the arch (Figs. 1(a) and (b)) or vertical load applied to 1/4 of the span of the structure (Figs. 1(c) and (d)). For a given arch, the latter load condition is the most unfavorable (Valluzzi *et al.* 2001).

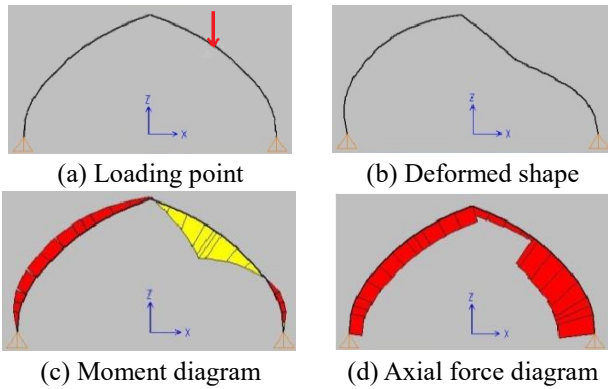


Fig. 2 Static analysis of mentioned arch

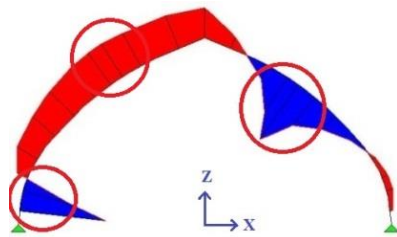


Fig. 3 Pressure line of the arch

Loading point, deformed shape, moment diagram and axial force diagram are shown in Fig. 2. According to Fig. 2(c), bending moment at the loading point is positive and maximum. On the other hand, based on Fig. 2(d), the axial force is in the form of pressure. If the ratio of the axial force over bending moment, is greater than  $h/6$  ( $h$  is the thickness of the vault), the stretch is created in the section, but if the ratio is smaller than  $h/6$ , the pressure will be created. In this area, the ratio is much larger than the  $h/6$  (6 cm) and stretch is created in the section and because of the positive bending moment in this area, the bottom of the arc placed in stretch and cracks at the bottom of the arch began to grow. The same mechanism occurs in a point on the opposite side of the load, with a negative moment the cracks are created on the top of the arch. The locations of the cracks in model and experiments are almost the same. Fig. 3 shows the pressure line of the arch. The eccentricity can be calculated as a ratio of the bending moment to the axial force at each point and the arch pressure profile is achieved by connecting the eccentricity points. According to this figure, another crack occurs close to the springer.

### 2.2 Reinforced masonry vaults

The application of FRP strips at the intrados or the extrados of the vaults alters the formation mechanism of the plastic hinges (Valluzzi *et al.* 2001). In the sections (which are in combined compressive and bending stresses), as for concrete structures, the resistance depends on the masonry compression strength and the fiber tensile strength.

Fig. 4 shows thrust line of the reinforced vault in the case of external strengthening. According to Fig. 4(a), the line of thrust can fall outside the lower edge of the vault without any structural collapse. For a vertical load applied to 1/4 of the structure span, the hinge formation in point B

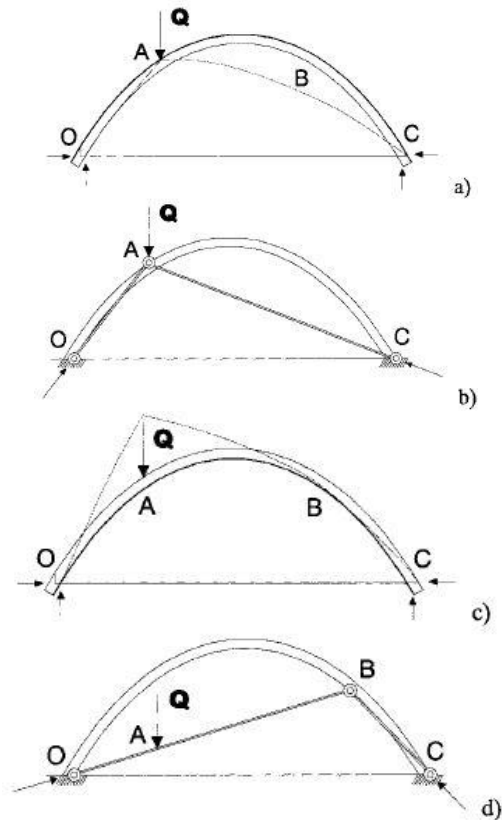


Fig. 4 Line of thrust and the static scheme of the reinforced vault at: (a, b) extrados; (c, d) intrados (Valluzzi *et al.* 2001)

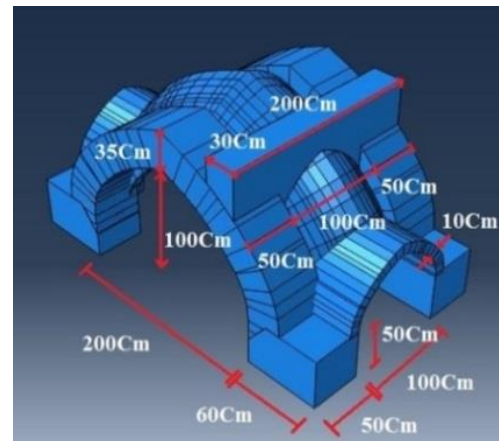


Fig. 5 Geometry of structure and load condition

is prevented. As a consequence, the vault becomes an isostatic structure (Fig. 4(b)). In the case of a structure reinforced at the intrados, Fig. 4(c), the line of thrust falls outside the upper edge of the structure and the fibers prevent the hinge formation close to the point of the load application (Fig. 4(d)).

### 3. Experimental model

In most of the studies, a single sheet with the circular arch is tested. However, the tested structures in this study are in the actual scale and more complex and are designed



(a) Installation of the plaster stencil as a template



(b) Full view of the vault and the rib cover

Fig. 6 Construction processes of the vault and the rib cover

according to the historical Iranian arches. In the first experiment, a structure without the reinforcement is tested and according to the test results, the second structure was reinforced using the CFRP and the same test is done to the effect of reinforcement.

### 3.1 The structural masonry arches (vault and rib cover)

The intended structure in this study consists of a vault and rib cover (Fig. 5).

Arch is six-part (with different radii). The clear span and height at the intrados are 200 cm and 100 cm, while the width of vault and rib cover are, 50 cm and 100 cm respectively. Also, the thickness of vault and rib cover is, 35 cm and 10 cm respectively. To connect arch to the rigid foundation, reinforced concrete foundations with dimensions of 50 cm×50 cm×40 cm is used. Reinforced concrete foundations with a slope of approximately 45 degrees have been made to prevent the possible bottom horizontal displacement of the vault. To implement this type of arch, the arch traced on the ground and then plaster stencil implemented. Plaster stencils have no structural function and only used to model the vault and the rib cover. Fig. 6(a) shows the plaster stencil. After installing plaster stencil at the beginning and end of the base, the vaults were built by pressure bricks and mortar contains gypsum, soil, and water. Each structure has four vaults and one rib cover. After completion of all the vaults, the rib covers are covered with brick and mortar. The rib covers are made with two arches, as a kind of dome. Fig. 6(b) shows the complete structure. In the reinforced structures, to have a better reinforcement, FRP fibers must be placed on a perfectly smooth surface. Due to the uneven surfaces vault and rib



(a) Application of thin layer of primer to the surface



(b) Installing CFRP



(c) Structures view after reinforcement

Fig. 7 Stages of structural strengthening

cover, the cement-sand mortar with the thickness of 4 cm used to make the surface as smooth as possible. The upper and lower vault and only the upper surface of the rib cover are cemented.

CFRP strips with the width of 40 cm are attached using a layer of primer in the extrados and intrados of the vault. Also, CFRP strip with the width of 20 cm is attached in the center of the rib cover (Fig. 7).

### 3.2 Characterization of the materials

The mechanical properties of each structure are highly dependent on the mechanical characteristics of all materials that are used to construct the structure. This section describes the mechanical characterization of the materials which are used in the brick masonry structure and the reinforcement system.

#### 3.2.1 Characterization of masonry mortar

The arches were constructed using a hydraulic mortar contains gypsum, soil, and water. To obtain the mechanical properties of the compressive strength tests (Fig. 8(a)) were performed according to the ASTM C472\_99 (2009). Compression tests were performed on six specimens. The compression strength is equal to 5.70 MPa.



(a) Mortar tests



(b) Masonry test specimens (triplet)



(c) Compression bricks test

Fig. 8 Determination of compressive strength

Table 1 Characteristics of the FRP strips

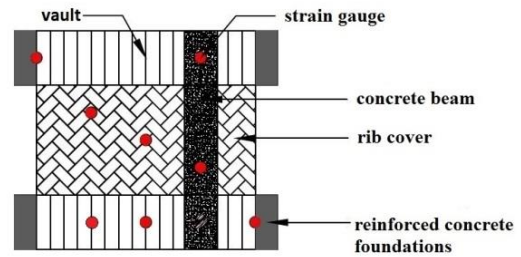
Characteristic	Reinforcement type
	CFRP(200)
Tensile strength (MPa)	4950
Elastic modulus (GPa)	240
Areal weight (gr/m <sup>2</sup> )	200
Thickness (mm)	0.111
Ultimate strain (%)	1.5

Table 2 Characteristics of the primer

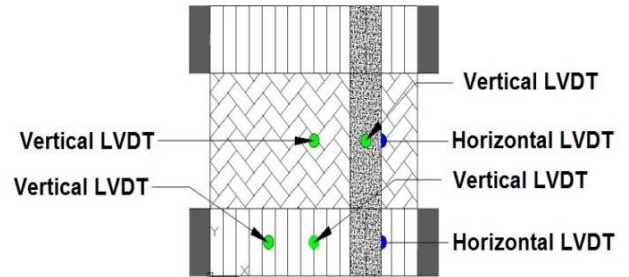
Description	Value
Colour	Concrete grey (mixed)
Density (at 25 0C)	1.65 kg/l (mixed)
Bonding Strength	> 3.5 MPa (concrete failed)
Compressive strength	95 MPa (7 days) at 35 0C
Tensile & Flexural Strength	> 30 MPa
Shear Strength	20 MPa
Full cured	After 7 days (at 25 0C)
Working Time	60 min. (25 0C)

### 3.2.2 Characterization of the bricks

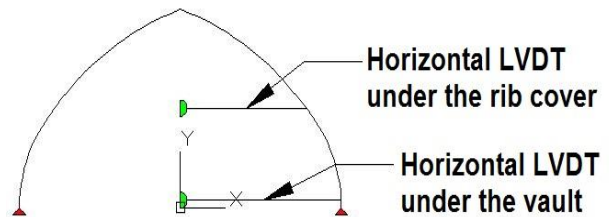
The solid clay bricks (220×110×70 mm<sup>3</sup>) were used for the construction of the masonry arches. The mechanical



(a) Strain gauges disposition along the vault and rib cover in top view of the tested structure



(b) LVDT position in Structure plan



(c) LVDT position in Structural section

Fig. 9 Measurement systems distribution in the test setup

properties of the bricks are obtained with testing six samples based on ASTM C1314-03b (2003). Uniaxial compression tests (Fig. 8(b), (c)) shows a mean strength variation of 22.50 Mpa for the bricks test and 11.20 MPa for the triplet.

### 3.2.3 Characterization of the reinforcement

Table 1 summarizes the geometrical and mechanical properties of the CFRP strips.

Table 2 shows the characteristics of the primer that is used to bond the FRP with the brick.

### 3.3 Test equipment

As shown in the Fig. 9, a concentrated load is applied to a quarter of the clear span, using a jack placed in series with a load cell of 250 kN capacity and distributed on the structures by a concrete beam. Eight strain gauges are placed on the CFRP material in reinforced structure and in the unreinforced structure, they placed along the brick (Fig. 9(a)). In each structure, eight linear variable differential transformers (LVDTs) were used to measure the displacement (Fig. 9(b), (c)).

Fig. 10 shows the test setup. The test setup is primarily consisting of a reinforced concrete footing and horizontal



Fig. 10 Test setup



(a) Cracks with a cross shape in the rib cover under a load of 137 kN



(b) Longitudinal crack on the top of the rib cover after loading.

Fig. 11 Cracks in the unreinforced rib cover

hydraulic jack and vertical hydraulic jack. These hydraulic jacks were fixed to a frame which was designed so that the maximum deformation under a prospective maximum load would be negligible. A data-logger system was used to display, monitor and record the load and displacement and strain measurements in real time during the test.

#### 4. Test results

In the following, the results of two tests on the non-reinforced and reinforced arches are proposed.

##### 4.1 Experimental investigation of unreinforced structure

To do the test, the steady pace load will be increased



(a) Cracks in the vault under the load of 152 kN



(b) Cracks in the vault under the load of 171 kN

Fig. 12 Cracks in the unreinforced vault.

gradually. Fig. 11 shows the cracks in the unreinforced rib cover. The first cracks with a cross shape in the rib cover were created at the load of 137 kN (Fig. 11(a)). The longitudinal cracks on the top of the rib cover can be seen in the final stage (Fig. 11(b)).

Fig. 12 shows the cracks in the unreinforced vault. With increasing the load up to 152 kN, a crack was seen in the vault that was started from the top of the vault (Fig. 12(a)). As a consequence of increasing the load up to 171 kN, another crack was seen in the vault (Fig. 12(b)). This crack, unlike the previous crack, was created in the bottom of the vault. Two plastic hinges in the vault, are important mechanisms that created in the structure. The locations of the cracks in model (Fig. 3) and experiments are almost the same. With an increasing load, the structure reaches ultimate capacity.

Fig. 13(a) and (b), show the crushed materials at the closest point to the spring. At this load level, the width of the cracks in the vault will be increased (Fig. 13(c) and (d)) and some cracks can be seen at the closest point to the spring. The unreinforced arch showed a brittle failure, due to the four hinges mechanism as predicted in Foraboschi (2004) and Borri *et al.* (2009). As it is clear in Figs. 13(a) and (b), cracks near the springer have been created but the sliding between brick and mortar is not created, based on Borri *et al.* (2009) and ASTM C 1314-03b (2003) the sliding occurs between brick and mortar in the first joint closest to the springer.

##### 4.2 Experimental investigation on reinforced structure

Based on the test results of the unreinforced structure, the cracks were created in the bottom and top of the vault. Therefore, strengthening the upper and lower the vault will



(a) Cracks at the closest point to the spring



(b) Cracks at the closest point to the spring



(c) Increase the width of the cracks in the right vault to 2 cm



(d) Increase the width of the cracks in the left vault to 2 cm

Fig. 13 Cracks in the structure in the ultimate capacity

be helpful. Fig. 14 shows the cracks in the rib cover as a result of the applied load for the reinforced structure. The first crack around the reinforced area in the rib cover was created under a load of 215 kN (Fig. 14(a)). With the load



(a) Crack around the reinforced area with FRP under the load of 215 kN



(b) Cracks at the junction of rib cover to the vault under the load of 235 kN

Fig. 14 Cracks in the rib cover as a result of the loading



(a) Cracks in an intermediate point on the opposite side of the load



(b) Cracks in the vault under the load of 245 kN

Fig. 15 Cracks in the vault under the loading



Fig. 16 Cracks at the junction of FRP to vaults under the load of 251 kN



Fig. 18 Crack in the rib cover of reinforced structure after loading



(a) FRP cement sand mortar separated from the rib cover



(b) The width of the cracks in the vault

Fig. 17 Cracks in the reinforced structures in ultimate capacity



(a) Place of cracks in the vault, unreinforced structure



(b) Place of cracks in the vault, reinforced structure

Fig. 19 Crack in the vault of (a): unreinforced structure and (b): reinforced structure

increasing up to 235 kN, cracks were created at the junction of the rib cover and vault (Fig. 14(b)). As a result of load increase to 245 kN, there was a clearance of 10cm between the created crack and the reinforced area.

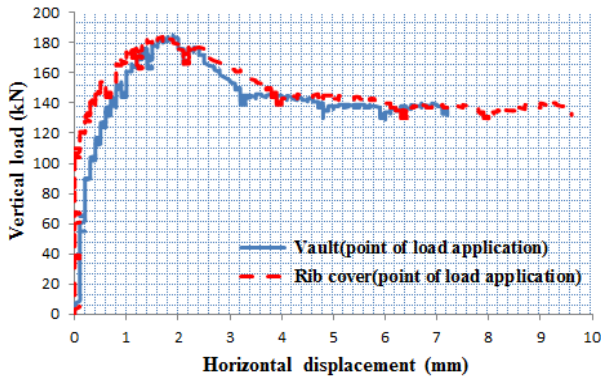
Fig. 15 shows the cracks in the vault under the loading. According to this figure, the pattern of cracks in the structure is uniform that reveals the uniform load distribution on the structure (Fig. 15(a) and (b)). With increasing load up to 251 kN, Fig. 16 shows the cracks were created at the junction of FRP to vaults created. In Milani *et al.* (2014), the sample had been reinforced locally inside and outside the arc. In Milani *et al.* (2014), the plastic hinge was reported under the load, on springer and in an intermediate point on the opposite side of the load. In this experiment, the detachment of FRP under the vault was not observed. In experiments such as Valluzzi *et al.* (2001), the sample was only reinforced in the intrados, the failure occurred because of the detachment of the fibers from the masonry close to the point of application of the load. Also, unlike the results observation, Foraboschi (2004) and Borri

*et al.* (2009), the sliding between brick and mortar in the first joint closest to the springer does not occur.

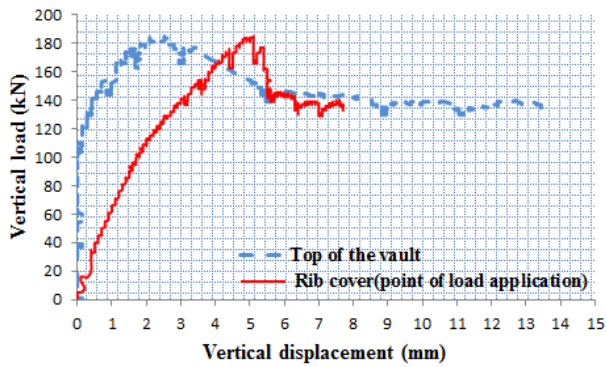
At this stage, the structure up to ultimate capacity and as a result, the width of the cracks increased and FRP connectivity boundaries to rib cover broken up. The width of the cracks in the vault increased up to 1 cm. Cracks in the rib cover was created in the form of zonal and meridional. Also, smaller vaults that transfer part of the load to the reinforced concrete foundations were damaged and cracks were transferred to the reinforced concrete foundations. Fig. 17 shows the cracks in the reinforced structures in ultimate capacity.

## 5. Result comparison between the Unreinforced and reinforced samples

In the unreinforced structure, the first cracks with a



(a)



(b)

Fig. 20 Load-displacement curve of the unreinforced structure, (a): horizontal, (b): vertical

cross shape in the rib cover were created under the load of 137 kN while in reinforced structures, the first crack around the reinforced area in the rib cover were created under a load of 215 kN.

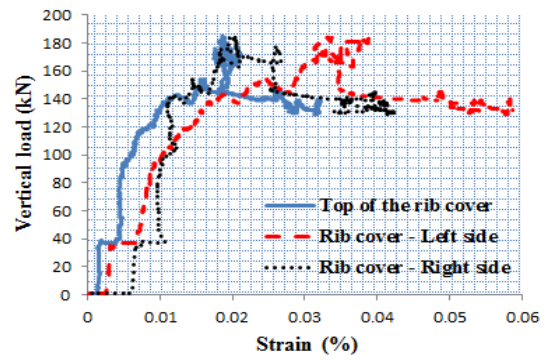
Moreover, the cracks in the unreinforced rib are created on the top of rib cover, but for the reinforced rib, the cracks moved towards the bottom of the reinforced area and led to the vaults. Fig. 18 shows the crack in the rib cover of reinforced structure after loading. Cracks in the vault of the unreinforced structure were created under the load of 152 kN.

However, the cracks were created in the vault of reinforced structures under the load of 245 kN. With increase in the length of the FRP strips up to the size of the vault, the capacity of tested structure will be enhanced and the cracks will moved toward the reinforced concrete foundation. Fig. 19 shows the cracks displacement as a consequence of the reinforcement.

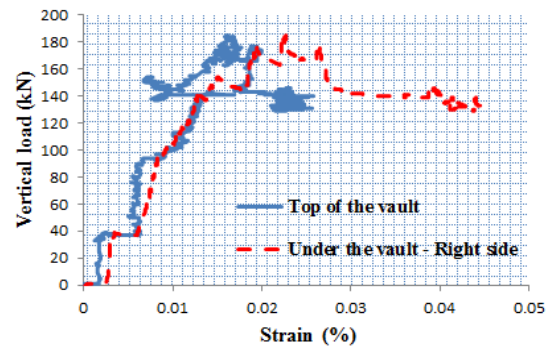
### 5.1 Unreinforced structure

Fig. 20 shows the load-displacement curves of the unreinforced structure. According to Fig. 20, in the vertical direction, the stiffness of the top of the vault is more than to the rib cover but in the horizontal direction, there is no significant change. The strain gage is located in the compression zone at the lower part of the vault.

The maximum range of this recorded strain is 0.000411 and the equivalent stress is 1.69 Mpa. This implies that the

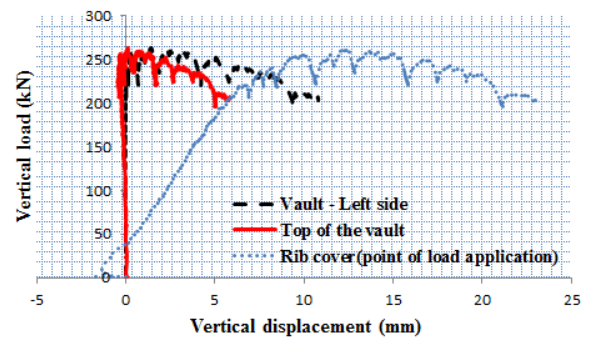


(a)

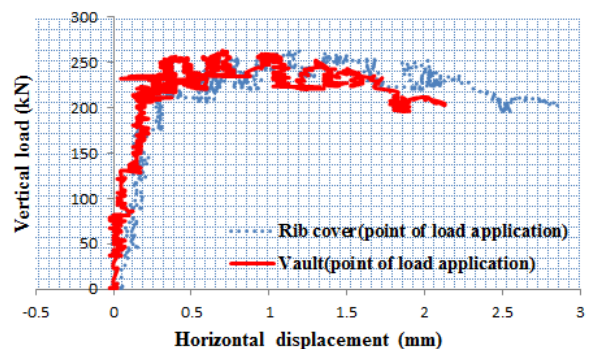


(b)

Fig. 21 Load-strain curve of unreinforced structure for (a): rib cover, (b): vault



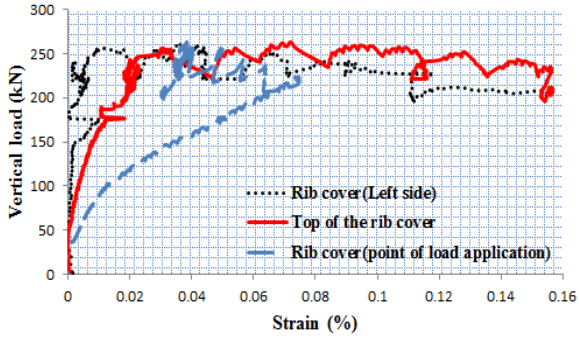
(a)



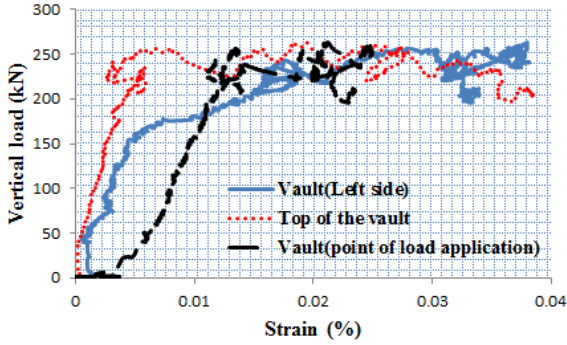
(b)

Fig. 22 Load-displacement curve of reinforced structure, (a): vertical (b): horizontal

bricks in this area are in linear phase. For this reason, the destruction did not happen on bricks of the lower part of the

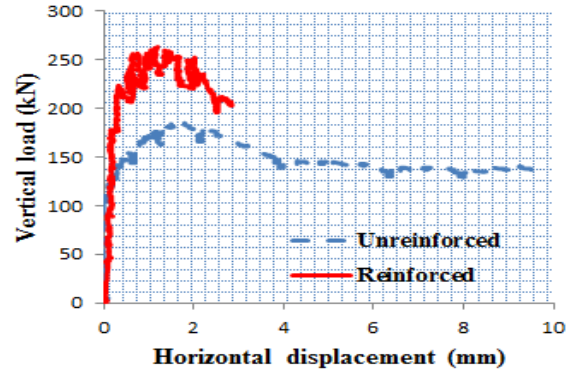


(a)

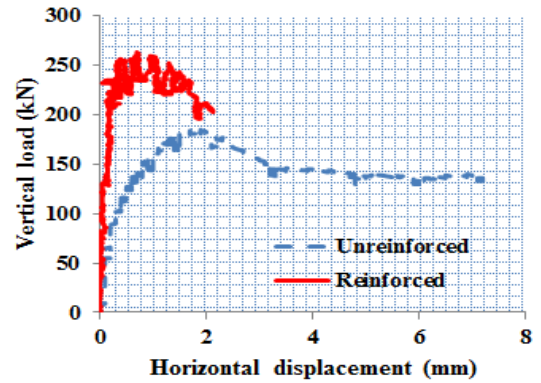


(b)

Fig. 23 Load-strain curve of reinforced structure for (a): rib cover, (b): vault

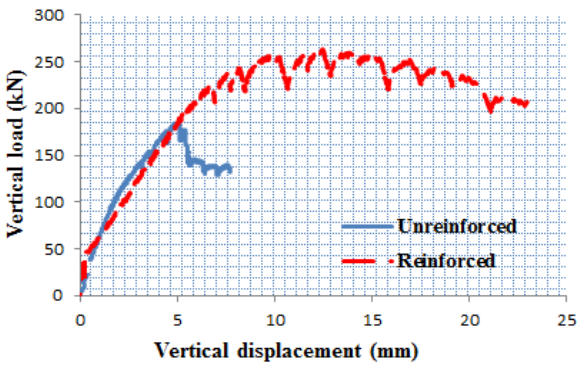


(a)

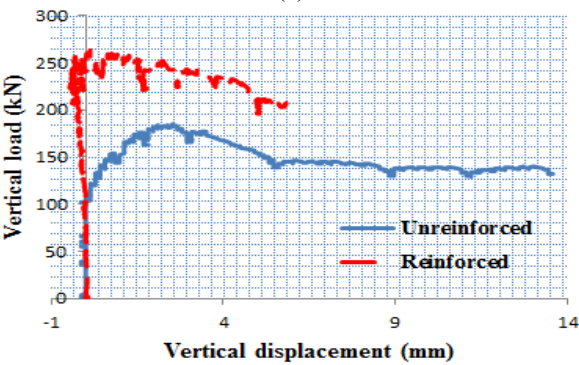


(b)

Fig. 25 Load-horizontal displacement curve of (a): rib cover, point of load application (b): vault, point of load application

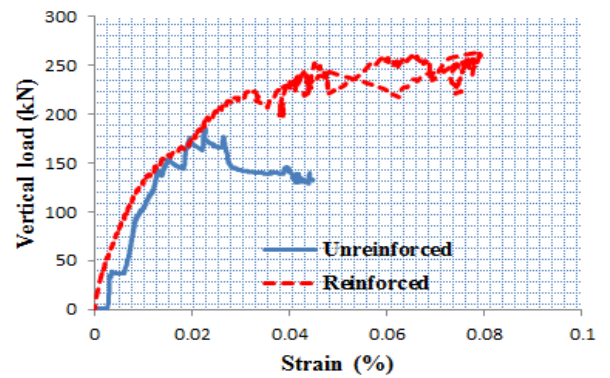


(a)

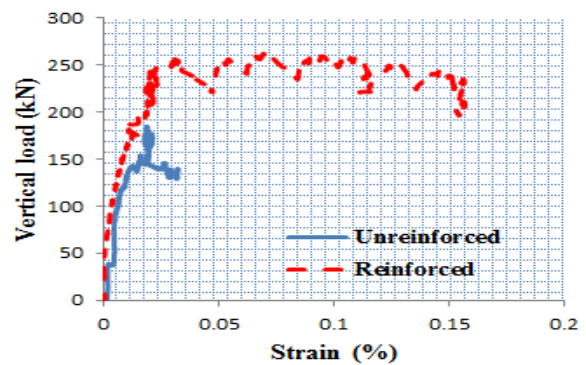


(b)

Fig. 24 Load-vertical displacement curve (a): rib cover, point of load application (b): top of vault



(a)



(b)

Fig. 26 Load-strain curve of (a): under the vault, right side, (b): top of the rib cover

vault. The strain gauges were installed in the tensile zone show that the bricks in this zone are in the non-linear phase.

Table 3 Structural response of ultimate load

Specimen	Ultimate load capacity (kN)	Load point deflection (mm)	Mode of failure
Unreinforced structure	181	2	Mechanism
Reinforced structure	251	10	Masonry crushing de-bonding

Strain gauges have been installed at the left of rib cover with a maximum recorded strain is equal to 0.000587 represents the non-linear behavior.

Fig. 21 shows the load-strain curves in different parts of the structure.

## 5.2 Reinforced structure

Fig. 22 represents the load-displacement curve for the reinforced structure. According to this figure, the displacements for the vaults are less than the same parameter for the rib cover. This means that the vaults are much stronger than rib covers. The movement in the middle and at a quarter of the span is almost identical, but failure and crack do not happen in the middle of the span. According to the Fig. 22(a), the stiffness of rib cover is less than the vault that means the rib cover requires more strengthening.

Fig. 23 shows the load-strain curve of reinforced structure. According to Fig. 23, a maximum strain recorded by the strain gauge is 0.0015 that means a stress of 360 Mpa in the FRP. It was much smaller than the tensile strength (4950 Mpa) and it shows that the FRP is still in a linear phase. But the bricks and the masonry materials are in the non-linear phase.

According to Fig. 23(a), the maximum strain is created in the spring. According to Fig. 23(b), the strain in the vault (right side) is negligible which causes less damages in the right side of the vault. Fig. 24 shows the comparison of the load-vertical displacement curve between the reinforced and the unreinforced structures.

Once the structure has been reinforced, the displacement decreased almost 70 percent that indicates an increase in the bearing capacity of the structure.

Fig. 25 shows comparison the load-horizontal displacement curve for the reinforced and the unreinforced structures. According to this figure, it can be concluded that the stiffness and the strength of the reinforced structure, in comparison with the unreinforced structure, increased and the displacement decreased.

Fig. 26 compares comparison the load-strain curve between the reinforced and the unreinforced structures. According to this figure, respectively, the ductility of the reinforced vault is more than the same value for the vault without reinforcement and the ductility of reinforced rib cover is larger that of the rib cover without reinforcement.

Table 3 summarizes the results of the tests on the unreinforced and reinforced structures.

## 6. Conclusions

The study was conducted on the arches, which are

historical structures that used mostly in Iran. The intended structure in this study consists of a vault and rib cover. The arc is six-part and solid clay bricks with hydraulic mortar contain gypsum, soil, and water were used for the construction of the masonry arches in the actual size. This study is a comparison between the structure without reinforcement and a structure that is reinforced with the CFRP strips. To do the reinforcement, the unreinforced structure is tested with the uniform vertical load and based on the test results, the other sample is reinforced with CFRP stripes. As it is clear for the unreinforced structure, in the point of load application, the stretch was created in the bottom of the arch and in a point on the opposite side of the load, the stretch was created in the top of the arch. Therefore, strengthening the upper and lower the vault will be helpful. Also, the rib cover capacity is lower than the vault, and as a result, it should be reinforced with the CFRP strips. The mechanism of the cracks creation in as a result of load, are discussed for the unreinforced sample and based on that, the appropriate points for CFRP stripes are selected.

For the reinforced sample, the expected fractures were created mainly between brick and mortar. If all the vaults and two directions of rib cover were reinforced, the structure loading capability will increase. Vaults have been much stronger than the rib cover and less displacement than rib cover and strengthening in the rib cover is more essential. The main difference between reinforced structure and unreinforced structure are movement of plastic hinges and delay in creation of plastic hinges and increasing ductility. With structural strengthening, bearing capacity increased by about 35%.

## Acknowledgments

The authors have to express out appreciation to Dr. Mohammad Mehdi Heydari for his assistance during the paper submission.

## References

- ICOMOS (2003), *International Scientific Committee for Analysis and Restoration of Structures of Architectural Heritage*, Recommendations for the Analysis, Conservation and Structural Restoration of Architectural Heritage, Guidelines of ICOMOS 14th General Assembly, Victoria Falls, Africa.
- Fanning, P. and Kelly, O. (1999), "Shear strengthening of reinforced concrete beams: An experimental study using CFRP plates", *Proceedings of the Structural Faults + Repair 99 Conference*, London, U.K., July.
- Nanni, A. (1993), *Fiber Reinforced Plastic Reinforcement for Concrete Structures: Properties and Applications*, Amsterdam, the Netherlands, Elsevier.
- Smith, S.T. and Teng, J.G. (2002), "FRP-strengthened RC Beams. I. Review of Debonding Strength Models", *Eng. Struct.*, **24**(4), 385-395.
- CNR-DT 200 (2004), *Guide for the Design and Construction of Externally Bonded FRP Systems for Strengthening Existing Structures*.
- Lourenço, P.B. and Oliveira, D.V. (2006), "Strengthening of masonry arch bridges: Research and applications", *Proceedings*

- of the 1st International Conference on Advances in Bridge Engineering, *Bridges-Past, Present and Future*, Brunel University, London, U.K., June.
- Valluzzi, M.R., Valdemarca, M. and Modena, C. (2001), "Behaviour of brick masonry vaults strengthened by FRP laminates", *J. Compos. Constr.*, **5**(3), 163-169.
- Foraboschi, P. (2004), "Strengthening of masonry arches with fiber-reinforced polymer strips", *J. Compos. Constr.*, **8**(3), 96-104.
- Creazza, G., Saetta, A.V., Matteazzi, R. and Vitaliani, R.V. (2001), *Analysis of Masonry Structures by FRP*, Historical Construction, In: Lourenço PB, Roca P, editors. Guimarães.
- Capozucca, R. (2007), "Behaviour of CFRP sheets bonded to historical masonry", *Proceedings of the Asia-Pacific Conference FRP in Structures*, Hong Kong.
- Aiello, M.A. and Sciolti, M.S. (2008), "Analysis of bond performance between FRP sheets and calcarenite stones under service and ultimate conditions", *Int. Masonry Soc.*, **21**(1), 15-28.
- Basilio, I., Oliveira, D. and Lourenço, P. (2004), "Optimal FRP strengthening of masonry arches", *Proceedings of the 13th International Brick and Block Masonry Conference*, Amsterdam, the Netherlands, July.
- Borri, A., Casadei, P., Casadei, G. and Hammond, J. (2009), "Strengthening of brick masonry arches with externally bonded steel reinforced composites", *J. Compos. Constr.*, **13**(6), 68-75.
- De Lorenzis, L., Dimitri, R. and La Tegola, A. (2007), "Reduction of the lateral thrust of masonry arches and vaults with FRP composites", *Constr. Build. Mater.*, **21**(7), 1415-1430.
- Briccoli Bati, S. and Rovero, L. (2008), "Towards a methodology for estimating strength and collapse mechanism in masonry arches strengthened with fiber reinforced polymer applied on external surfaces", *Mater. Struct.*, **41**(7), 1291-306.
- Foraboschi, P. (2004), "Strengthening of masonry arches with fiber-reinforced polymer strips", *J. Compos. Constr.*, **8**(3), 96-104.
- De Lorenzis, L. and Zavarise, G. (2009), "Interfacial stress analysis and prediction of debonding for a thin plate bonded to a curved substrate", *Int. J. Non-Lin. Mech.*, **44**(4), 358-370.
- Greco, A. and Pau, A. (2011), "Detection of a concentrated damage in a parabolic arch by measured static displacements", *Struct. Eng. Mech.*, **39**(6), 751-765.
- Ataci, S., Tajalli, M. and Miri, A. (2016), "Assessment of load carrying capacity and fatigue life expectancy of a monumental Masonry Arch Bridge by field load testing: A case study of veresk", *Struct. Eng. Mech.*, **59**(4), 703-718.
- Xin, R., Yao, J. and Zhao, Y. (2017), "Experimental research on masonry mechanics and failure under biaxial compression", *Struct. Eng. Mech.*, **61**(1), 161-169.
- Eshwar, N., Ibell, T., Nanni, A. and Porter, A.D. (2005), "Effectiveness of CFRP strengthening on curved soffit RC beams", *Adv. Struct. Eng.*, **8**(1), 55-68.
- ASTM C 472-99 (2009), *Standard Test Methods for Physical Testing of Gypsum*, Gypsum Plasters and Gypsum Concrete, West Conshohocken, Pennsylvania, U.S.A.
- ASTM C 1314-03b (2003), *Standard Test Method for Compressive Strength of Masonry Prisms*, ASTM International, West Conshohocken, Pennsylvania, U.S.A.
- Milani, G., Fedeleh R., Lorencio, P.B. and Basilo, E., (2014), "Experimental and numerical FE analyses of curved masonry prisms and arches reinforced with FRP materials", *Proceedings of the 9th International Conference on Structural Analysis of Monuments and Historical Constructions*, SAHC, Mexico.
- Misseri, G. and Rovero, L. (2017), "Parametric investigation on the dynamic behaviour of masonry pointed arches", *Arch. Appl. Mech.*, **87**(3), 385-404.
- Dimitri, R. and Tornabene, F. (2015), "A parametric investigation of the seismic capacity for masonry arches and portals of different shapes", *Eng. Fail. Anal.*, **52**, 1-34.
- Rotunno, T., Rovero, L., Toniatti, U. and Bati, S.B. (2014), "Experimental study of bond behavior of CFRP-to-brick joints", *J. Compos. Constr.*, **19**(3), 04014063.
- Ghiassi, B., Oliveira, D.V. and Lourenço, P.B. (2014), "Hygrothermal durability of bond in FRP-strengthened masonry", *Mater. Struct.*, **47**(12), 2039-2050.

PL